Skeletal Radiol (2012) 41:137–148
DOI 10.1007/s00256-011-1291-3

REVIEW ARTICLE

High resolution magnetic resonance imaging of the patellar retinaculum: normal anatomy, common injury patterns, and pathologies

Shrey K. Thawait · Theodoros Soldatos · Gaurav K. Thawait · Andrew J. Cosgarea · John A. Carrino · Avneesh Chhabra

Received: 18 July 2011 / Revised: 19 September 2011 / Accepted: 22 September 2011 / Published online: 9 November 2011

Abstract The medial patellar retinaculum (MPR) and the lateral patellar retinaculum (LPR) are vital structures for the stability of the patella. Failure to identify or treat injury to the patellar retinaculum is associated with recurrent patellar instability and contributes to significant morbidity. High-resolution magnetic resonance imaging (MRI) readily depicts the detailed anatomy of various components (layers) of the retinacula. In this review article, we discuss normal anatomy, important landmarks, common injury patterns, and other pathologies encountered in patellar retinacula. High field strength MRI is an excellent noninvasive tool for evaluation of patellar retinaculum anatomy and pathology. This article will help the reader become familiar with normal imaging findings and the most commonly occurring injuries/pathologies in MPR and LPR.

Keywords Patellar retinaculum · Medial patellar retinaculum · Lateral patellar retinaculum · Medial patellofemoral ligament · Medial patellomeniscal ligament · Medial patellotibial ligament · Injury · Pathology · Magnetic resonance imaging

S. K. Thawait
Yale University - Bridgeport Hospital,
267 Grant Street,
Bridgeport, CT 06610, USA

S. K. Thawait
e-mail: sthawai2@jhmi.edu

T. Soldatos · G. K. Thawait · A. J. Cosgarea · J. A. Carrino · A. Chhabra
Johns Hopkins Hospital,
600 North Wolfe Street,
Baltimore, MD 21287, USA

T. Soldatos
e-mail: tsoldat1@jhmi.edu

G. K. Thawait
e-mail: gthawai1@jhmi.edu

A. J. Cosgarea
e-mail: acosgar@jhmi.edu

J. A. Carrino
e-mail: jcarrin2@jhmi.edu

A. Chhabra (✉)
Department of Radiology and Radiological Science,
The Johns Hopkins Hospital,
601 North Caroline Street, JHOC 3262,
Baltimore, MD 21287, USA
e-mail: achhabr6@jhmi.edu

Introduction

The patellar retinacula are thin ligamentous structures that extend obliquely and transversely from the patellar margins to the femur and tibia and provide substantial stability to the knee joint. Failure to identify or treat injury to the patellar retinacula is associated with recurrent patellar subluxations/dislocations, instability, and increased morbidity. Magnetic resonance (MR) imaging has been established as the modality of choice for the noninvasive evaluation of ligamentous injuries. With increasing use of high-field (1.5 T or higher strength) and high-resolution MR imaging techniques, the various layers of the patellar retinacula and their pathologic entities are readily demonstrated. This review illustrates the MR imaging features of the normal patellar retinacula, and their injury patterns and other miscellaneous pathologies involving them along with relevant case examples.

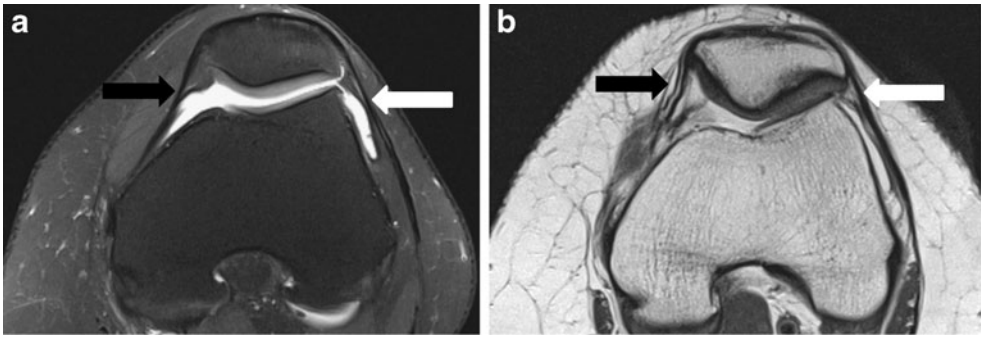

Fig. 1 Normal MR appearance of the patellar retinaculum in the upper part. **a** Axial proton density image with fat saturation and **b** axial proton density images show the MPR (*black arrow*) and the LPR (*white arrow*), seen as a discrete band of low SI on both images

Anatomic considerations and MR imaging technique

Fibrous connective tissue layers and condensations of tissue planes derived from the neighboring structures, such as collateral ligaments of the knee, form the medial and lateral patellar retinacula (MPR, LPR). The MPR and LPR extend obliquely and transversely from the medial and lateral patellar margins to the femur and tibia and, similarly to other ligamentous structures, they are depicted on MR images as discrete bands of low signal intensity on both T1- and T2-weighted images (Fig. 1). The complex anatomy of the MPR and LPR has been illustrated in detail by several recent anatomical dissection studies [1–4]. The MPR belongs to the medial capsular and supporting structures of the knee and is composed of the following three layers [5, 6], which are readily identifiable using high-resolution MR imaging (Figs. 2 and 3):

- Layer I, which receives contributions from deep crural fascia
- Layer II, which receives contributions from the superficial portion of the medial collateral ligament (MCL)
- Layer III, which receives contributions from the joint capsule; meniscofemoral and meniscotibial extensions of the deep portion of the MCL; and medial patellofemoral, medial patellomeniscal, and medial patellotibial ligaments from superior to inferior

Layers I and II fuse together along the anterior aspect of the medial side of the knee, whereas layers II and III fuse along the posterior aspect of the joint [5]. The medial patellofemoral, patellomeniscal, and patellotibial ligaments are thickenings of the joint capsule and are arranged according to their names at the respective levels of medial femoral condyle, medial meniscus, and medial tibial plateau from superior to inferior (Fig. 4). The medial patellofemoral ligament (MPFL) has been recognized as the primary passive restraint resisting lateral translation of the patella (Fig. 5) [4] and attaches at the saddle between medial epicondyle and adductor tubercle [7]. The MPFL is also the largest and clinically most important ligament of the medial retinaculum [8], and although not very thick, it has a surprisingly high tensile strength [4]. The MPFL is consistently identified in anatomic specimens [1] and is depicted on axial MR images as a low signal intensity band-like structure just deep and distal to the vastus medialis obliquus muscle [9]. The latter represents the distal fibers of the vastus medialis muscle, which have a more oblique or horizontal orientation to the main bulk of

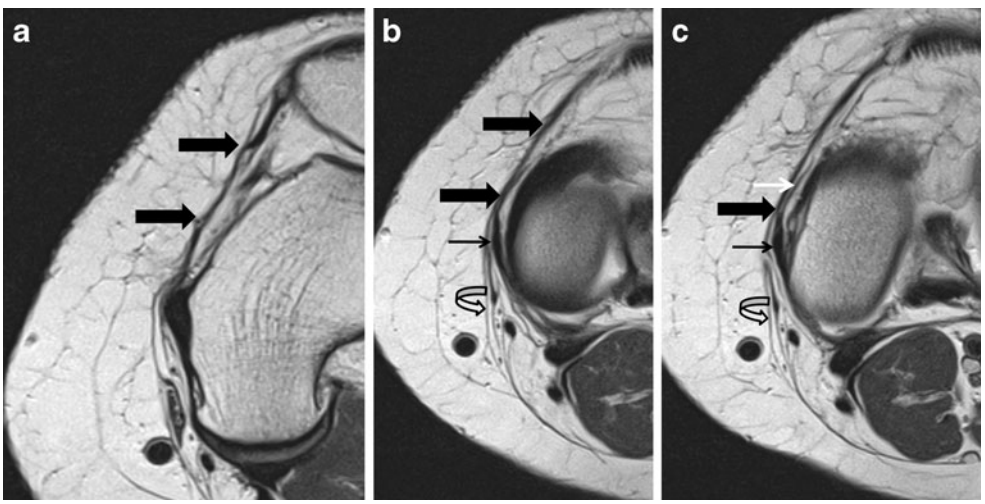

Fig. 2 Normal anatomy of the three layers of MPR. Sequential axial proton density images (**a**, **b**, and **c**) show the different components of the medial retaining structures. Layers I and II are fused anteriorly (*thick black arrows*). Layer I of the MPR continues posteriorly (*curved black arrow*). Superficial and deep portions of the MCL are also seen together (*thin black arrows*). Meniscofemoral extension of the deep MCL is demonstrated (*white arrow* in **c**)

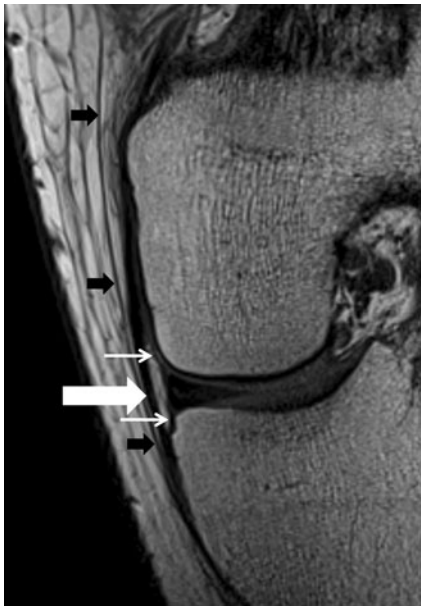

Fig. 3 Normal anatomy of the three layers of MPR as seen on a coronal proton density image. *Small black arrows* show the crural fascia which is considered as layer I of MPR. The *large white arrow* points to the MCL, which is considered as layer II of the MPR. Finally the *small white arrows* show the meniscofemoral (*superior white arrow*) and meniscotibial (*inferior white arrow*) ligaments. They are considered as extensions of the deep layer of MCL and constitute the deepest layer III

the muscle and enable medial translation and stabilization of the patella [10]. The distal margin of the vastus medialis oblique muscle attaches along the proximal margin of the MPFL [11]. The other distal-medial restraint to lateral patellar displacement is provided by the medial patellomeniscal ligament [12]. It is also located within layer III and is visible at the medial meniscal level as a hypointense taut band (Fig. 6a). The medial patellotibial ligament is a very thin structure within layer III and is visible on high resolution MR scan at the tibial plateau level (Fig. 6b). In a normal knee, this tri-layered MPR is relatively similar in thickness to the LPR.

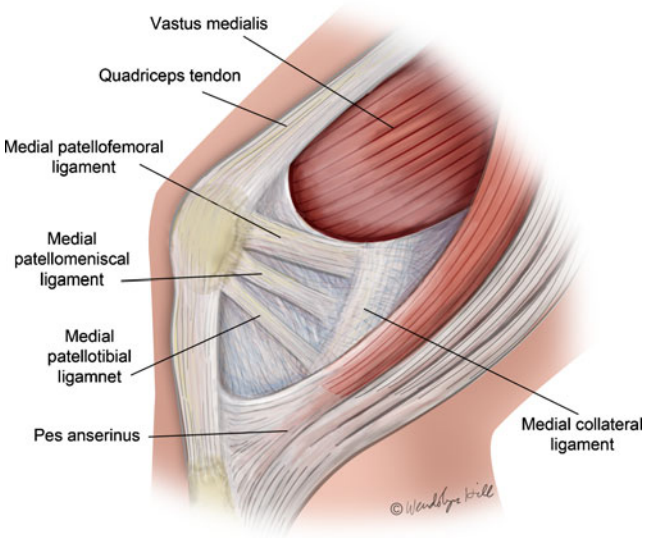

Fig. 4 Illustration showing the major supporting ligaments of the knee in the sagittal plane

In contrast to the MPR, the anatomy and biomechanics of the LPR are relatively less well understood (Fig. 7). The LPR is formed by several fascial layers on the anterolateral aspect of the knee joint [2] but is not perceived as a discrete anatomical unit due to the various converging and interdigitating structures and facial layers. Various distinct condensations of fibers have been postulated in the LPR: a broad tissue oblique band, which links the iliotibial band to the patella, and the three capsular ligaments, the patellofemoral (epicondylopatellar band), deep transverse band (patellomeniscal), and patellotibial ligaments [2]. However, the above condensations are not consistently visualized on MR images.

Table 1 demonstrates the typical protocol employed for the orthopedic imaging of the knee joint. Axial images are best for the identification of the individual components of the patellar retinacula, sagittal images are additionally suitable for the assessment of the patellomeniscal, patellotibial, and patellofemoral ligaments, whereas coronal images may be used to confirm the findings of the aforementioned planes. It may be speculated that additional diagnostic information will be available in the future through the increasing use of isotropic 3D imaging, which enables isotropic multiplanar reconstructions in arbitrary planes resulting in better axial and longitudinal display of various intricate layers of the retinacula.

MR imaging patterns of patellar retinaculum injuries

Acute injuries

The MPR is invariably injured in acute patellar subluxations/dislocations [13]. LPR injuries are frequently observed in direct trauma or in translational events associated with anterior cruciate ligament (ACL) injuries [8]. High-resolution MR imaging enables precise assessment of the location and grading of the retinacular injury. The retinacular tear should be assessed on the patellar attachment side, midportion and femoral attachment side in the axial planes, as well as from superior to inferior in the axial and sagittal planes for evaluation of injuries to the patellofemoral, patellomeniscal, and patellotibial ligament portions. The retinacular injury is graded in the same way as any other ligamentous injury, namely grade I (periligamentous edema), grade II (partial tear with edema-like signal within the ligament), and grade III (complete tear) (Fig. 8). Other associated common MR imaging findings

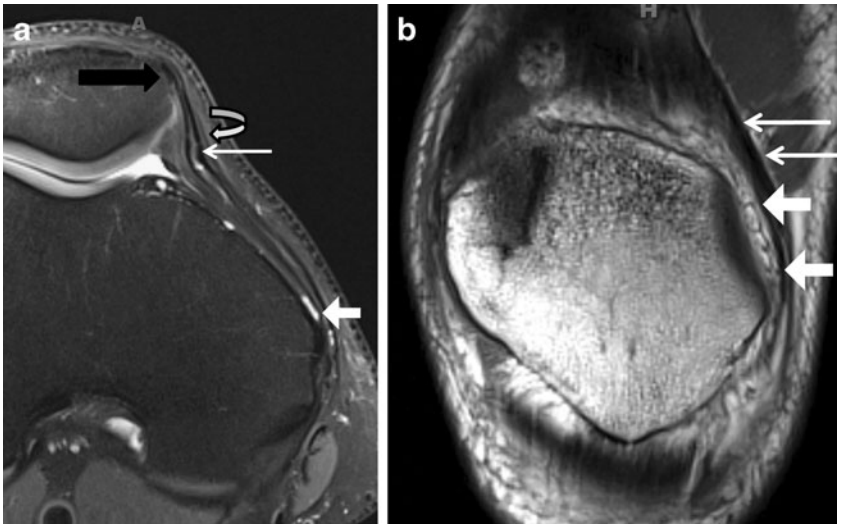

Fig. 5 Normal anatomy of MPFL. **a** Axial proton density image with fat saturation shows the patellar attachment at the superior medial border of the patella (*black arrow*). The femoral attachment is at the bony groove between the medial epicondyle and the adductor tubercle (*block white arrow*). The MPFL can be located just deep to the VMO muscle (*thin white arrow*). Also note the crural fascia, layer I of MPR (*curved arrow*). **b** Coronal proton density image shows the MPFL (*block white arrows*) just proximal to patellar attachment at the superior medial border of the patella. Also note the VMO tendon (*thin white arrows*)

include osteochondral injuries of the inferomedial patella, impaction-related contusions/subchondral fractures of the lateral femoral condyle, joint effusion, loose bodies, and capsular injury (Fig. 8) [9, 13–16]. The femoral origin of the MPFL is the most common site of injury and is also associated with less likelihood of regaining the pre-injury activity level [13, 17]. Various grades of stripping of MPR and LPR are commonly seen from their femoral insertions in ACL injury–related translational events, which should be recognized and reported. In addition, the vastus medialis oblique muscle is often injured, whereas the vastus intermedius and vastus lateralis are less commonly involved (Fig. 9) [13]. In some cases, the injury may be isolated to the inferior layers of the retinaculum, such as the medial patellomeniscal or medial patellotibial portions of the ligament (Figs. 10, 11). In the authors' experience these inferior ligaments may be injured in various combinations, especially in twisting injuries, where they may be associated with medial meniscal injuries and meniscocapsular sprains. Injury to the medial patellomeniscal ligament has recently been shown to lead to patellar instability [12]. The LPR is less commonly injured and may sustain disruption in cases of medial patellar dislocation, ACL injury, or by direct blow to the anterolateral knee [8]. Tight lateral patellar retinaculum (known as excessive lateral pressure syndrome) may cause abnormal lateral patellar tilt and exaggerated pressure in the lateral aspect of the patellofemoral joint, friction-related superolateral Hoffa's fat pad edema, and early patellofemoral osteoarthrosis [18, 19]. Surgical release of the LPR has been utilized to correct the

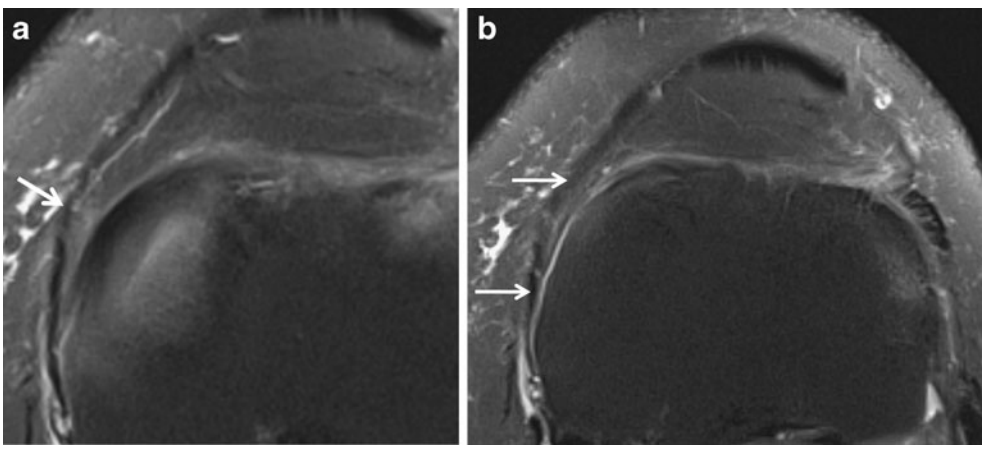

Fig. 6 Axial proton density image with fat saturation (**a**) at the level of the joint demonstrates normal medial patellomeniscal ligament (*arrow*). Another axial proton density image with fat saturation (**b**) at the level of the tibial plateau shows normal medial patellotibial ligament (*arrows*)

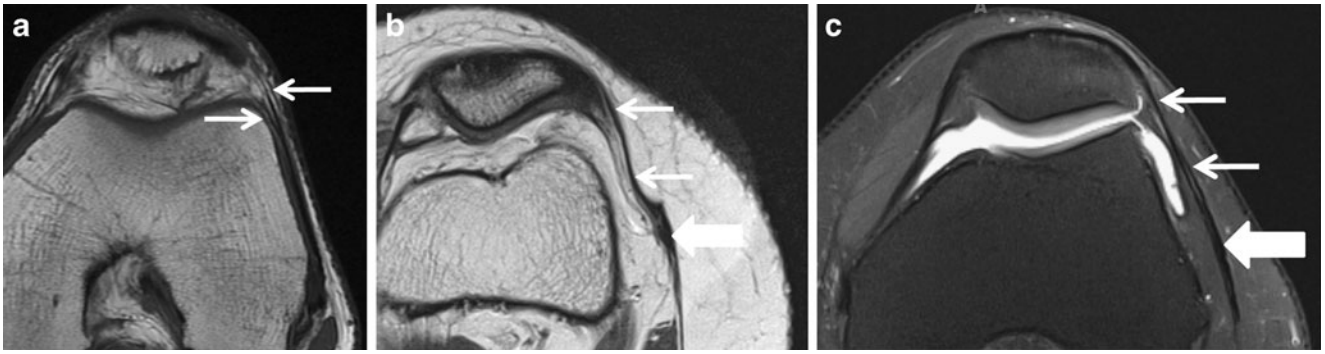

Fig. 7 Normal anatomy of the LPR (*thin arrows*) as seen on axial proton density image without fat saturation (**a** and **b**) and axial proton density image with fat saturation (**c**) from different subjects. Also note the iliotibial tract (*large arrow* in **c**)

Table 1 A typical knee protocol on a high field strength 3 Tesla magnet

Sequence	TR (ms)	TE (ms)	Echo spacing (ms)	Turbo factor	ST (mm)	Voxel size (mm)	Base resolution
T1 COR without FS	750	9.7	9.65	5	2	0.3×0.3×2	384
PD COR with FS	63	2	9.07	15	2	0.4×0.4×2	320
PD SAG with FS	3,940	54	9.07	15	2	0.4×0.4×2	320
PD SAG without FS	1,000	30	5.08	41	2	0.5×0.5×0.5	320
PD AX with FS	3,780	54	10.8	15	2	0.4×0.4×2	320
PD AX without FS	4,570	43	10.8	9	2	0.3×0.3×2	384

TR Time of repetition, *TE* time of echo, *ST* slice thickness, *Cor* coronal, *Sag* sagittal, *Ax* axial, *FS* fat saturation

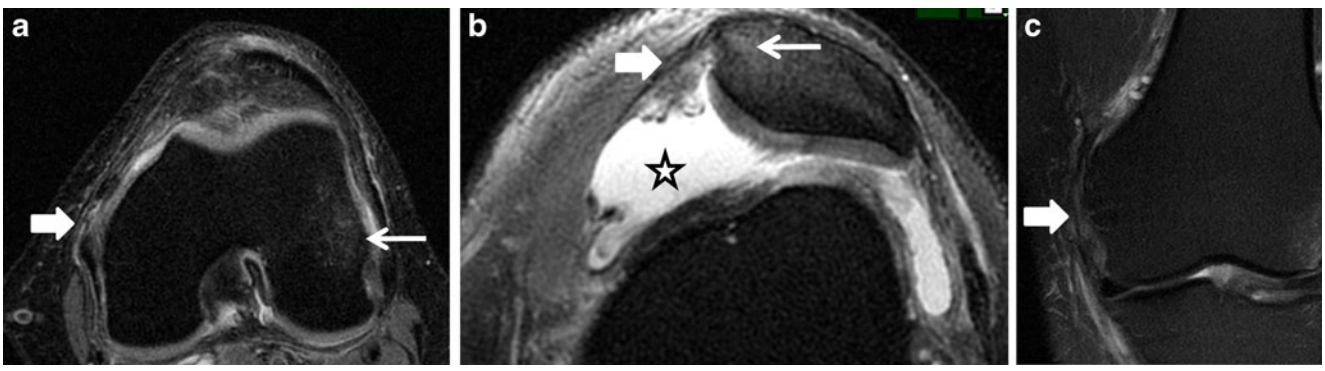

Fig. 8 A 33-year-old male with left knee pain. **a** Axial proton density image with fat saturation shows complete tear (grade III) of the MPR and MPFL from the femoral attachment (*thick arrow*). Bone marrow edema and subchondral fracture of anterior lateral femoral condyle (*thin arrow*) is also noted. **b** Axial proton density image with fat saturation at inferior level shows partial tear (grade II) of the patellar attachment of MPR (*thick arrow*) and bone marrow edema of the medial patella at the avulsion site of the MPR (*thin arrow*). Also note the joint effusion (*asterisk*) and lateral displacement of the patella. **c** Coronal proton density image with fat saturation redemonstrates complete tear (grade III) of the MPR from the femoral attachment (*thick arrow*)

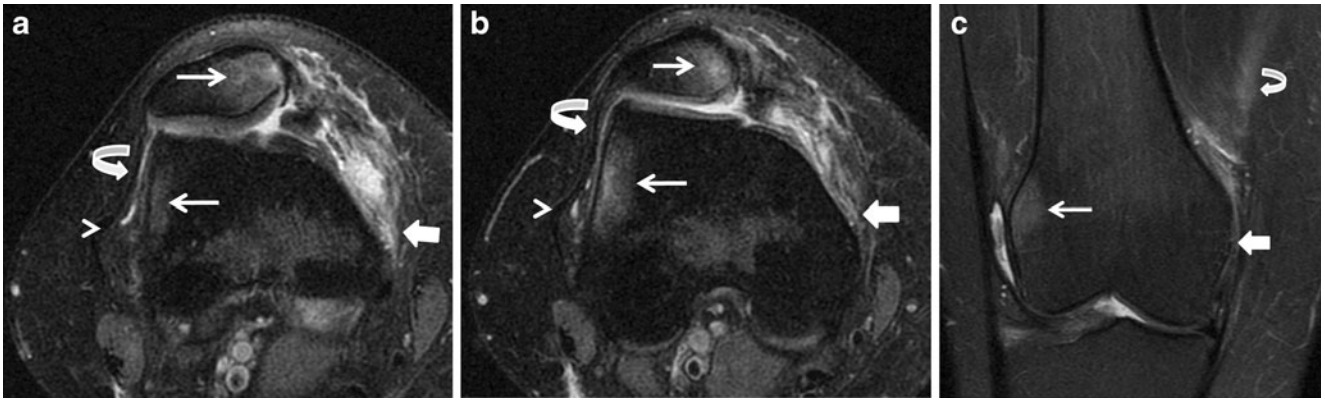

Fig. 9 A 23-year-old woman with history of patellar dislocation. Axial proton density images with fat saturation (**a**, **b**) show grade III tear of MPR and MPFL (*thick arrows*) and bone marrow edema of the medial patella and lateral femoral condyle (*thin arrows*). Note the normal structures on the lateral aspect, normal iliotibial tract (*arrowheads*), and normal LPR (*curved arrows*). Coronal proton density image with fat saturation (**c**) redemonstrates grade III tear of MPR and MPFL (*thick arrow*) and bone marrow edema of the lateral femoral condyle (*thin arrow*). Also note the grade I tear of VMO (*curved arrow*)

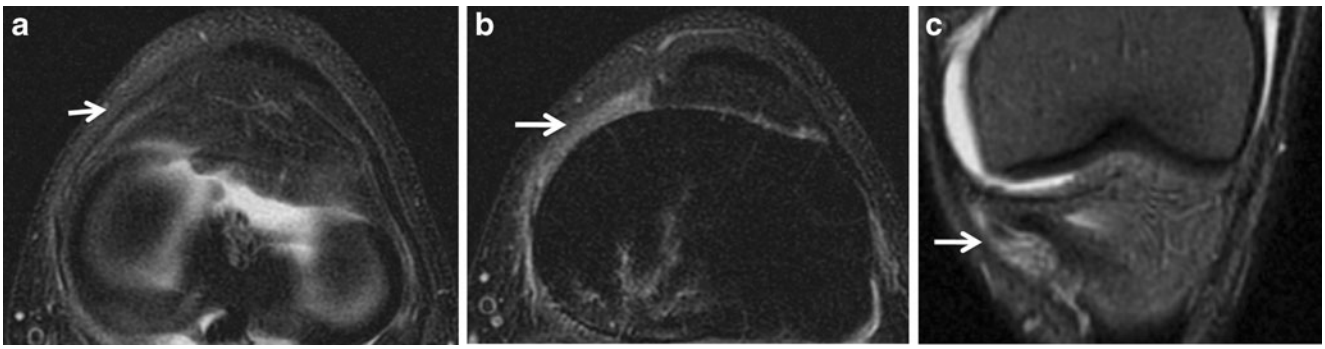

Fig. 10 A 20-year-old man with a twisting knee injury. **a** Axial proton density image with fat saturation shows grade I–II sprain of the medial patellomeniscal ligament (*arrow*). **b** Axial proton density image with fat saturation further distally. **c** Coronal proton density image with fat saturation shows grade II–III sprain of medial patellotibial ligament (*arrows*). The medial patellofemoral ligament was intact in this case (image not shown)

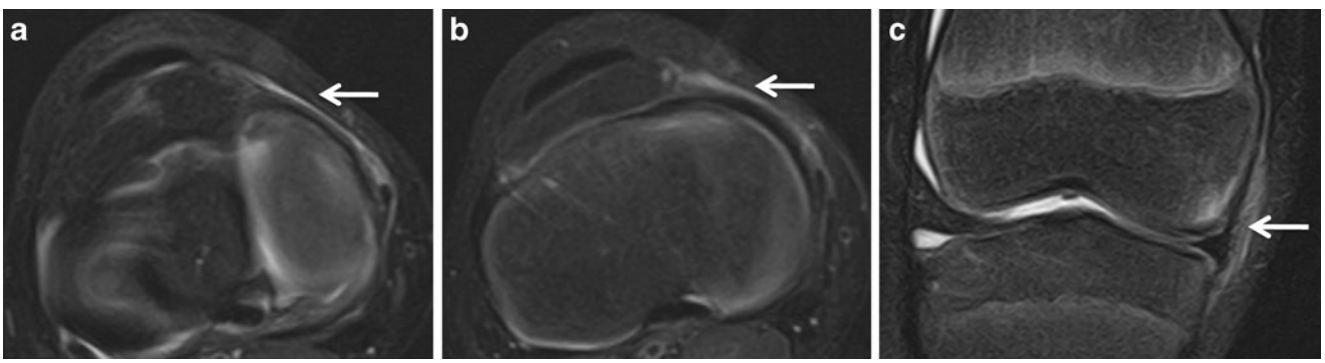

Fig. 11 A 12-year-old boy with knee pain after sustaining a twisting knee injury. **a** Axial proton density image with fat saturation shows grade I sprain of the medial patellomeniscal ligament (*arrow*). **b** Axial proton density image with fat saturation further distally. **c** Coronal proton density image with fat saturation shows grade II–III sprain of medial patellotibial ligament (*arrow*). The medial patellofemoral ligament was not injured in this case (image not shown)

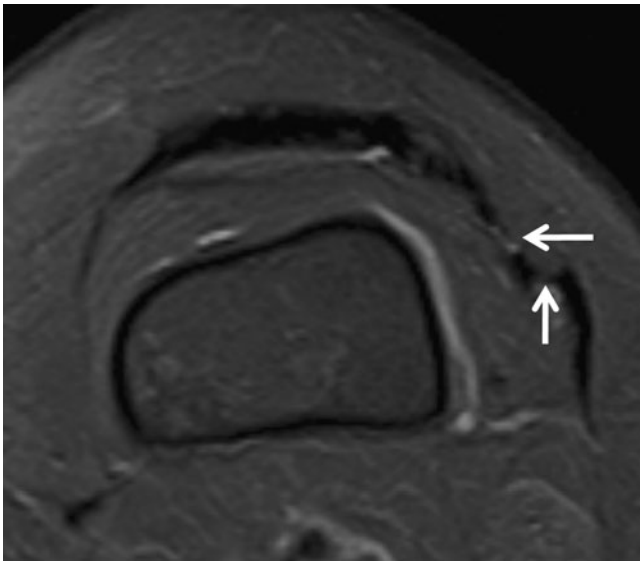

Fig. 12 A 25-year-old woman with history of prior knee surgery. Axial proton density image with fat saturation shows the postsurgical defects anteriorly in LPR (*arrows*)

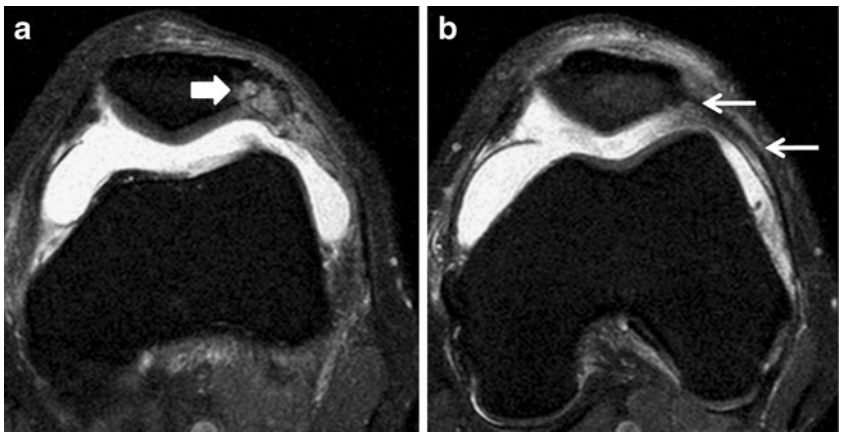

Fig. 13 A 34-year-old man who injured his knee 2 weeks prior while running, presented with pain, swelling, limited range of motion. Axial proton density images with fat saturation (**a**, **b**) images show bipartite patella with stress-related edema and cystic changes (*thick arrow*) and thickening and remodeling of the lateral retinaculum (*thin arrows*). Note that there is no frank disruption of the attachment of the lateral retinaculum at patella

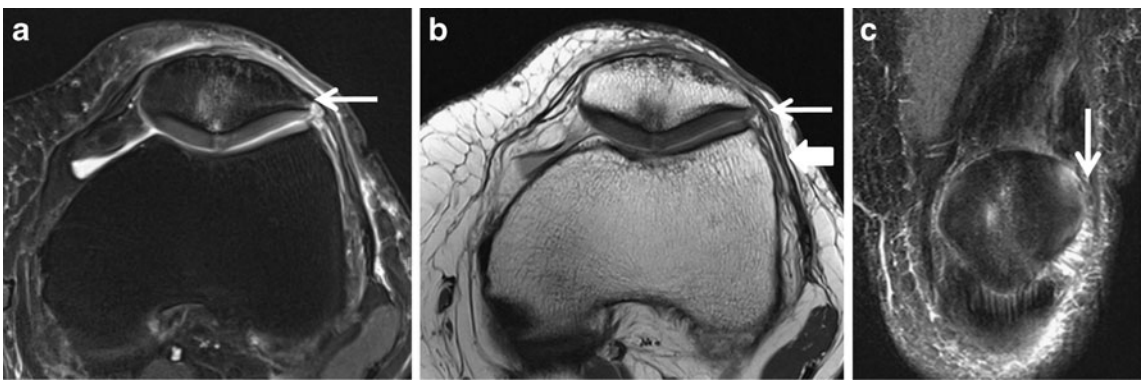

Fig. 14 A 59-year-old woman with old knee injury and known post-traumatic arthritis presents with worsening knee pain. Axial proton density image with fat saturation (**a**), axial proton density image (**b**), and coronal proton density image with fat saturation (**c**) show injury of patellar insertion of the lateral retinaculum (*thin arrows*) and thickened lateral retinaculum (*thick arrow*), consistent with history of old injury. Also note the minimal bone marrow edema changes of the patella, indicating chronic instability

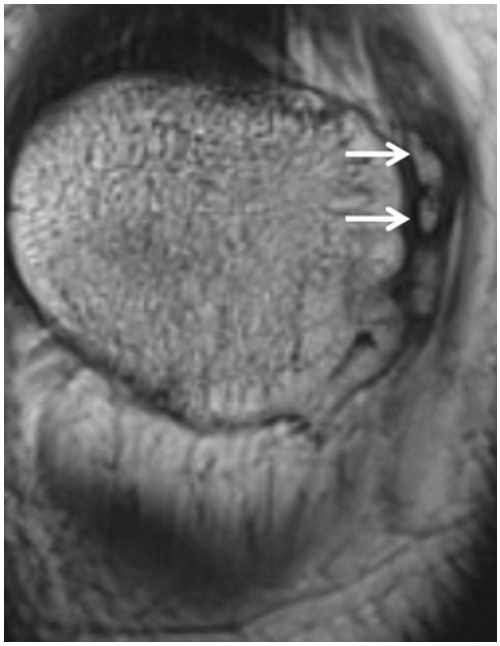

Fig. 15 A 36-year-old woman with old injury to the knee and intermittent knee pain. Coronal proton density image shows bony productive changes of the patella at the medial pole (*arrows*) consistent with chronic avulsive changes

above syndrome (Fig. 12), and an injured appearance of the retinaculum is more commonly due to this surgery rather than the aforementioned mechanisms [20].

Subacute and chronic injuries

Differentiation between subacute and chronic injuries by MR imaging alone may be difficult as there is some overlap, and clinical history is very helpful. Subacute injury manifests as a combination of resolving bone marrow and fascial edema, bony avulsive deformity at the retinacular attachments, and thickening/attenuation as well as remodeling of the retinaculum along its transverse span (Fig. 13). Sometimes, a subacute hematoma may be seen within the retinacular layers and may mimic a neoplastic lesion. Knowledge of the above lesion in the light of clinical history, especially with the presence of T1 hyperintensity or surrounding complete hypointense hemosiderin ring warrants a short-term follow-up to resolution, rather than a biopsy. Chronic/old injury manifests with one or more of the following findings: fibrosed/thickened/attenuated retinaculum (Fig. 14), bony productive changes at a retinacular attachment, and ossification of the retinacular layers (Fig. 15). In some chronic cases, altered stresses lead to thickening of the retinaculum on one side with attenuation of the contralateral retinaculum (Fig. 16). Additionally, synovial diverticulum or ganglion cyst may form due to the associated previous capsular injury, exiting from the layers of the retinaculum with or without communication with the knee joint space, respectively. Correct identification of the above lesions is essential, in order to avoid mistaking them for neoplasms. A synovial diverticulum is defined as a hernial protrusion of the synovial membrane of a joint or a tendon sheath. These protrusions are commonly encountered in the extremities (Fig. 17), but have been more widely reported in the spine, where they are more likely to cause nerve root compression [21]. Ganglion cysts are structures of unknown etiology, generally speculated to represent degenerated mucoid connective tissue, specifically collagen [22]. These benign cystic lesions may result from previous retinacular injury caused by various mechanisms such as patellar subluxation, knee arthroscopy, or direct injury (Fig. 18). A chronic hematoma in the retinaculum may also mimic a tumor. In appropriate cases, follow-up imaging is very helpful (Fig. 19).

Patellofemoral malalignment describes clinical abnormalities resulting from a complex constellation of static and dynamic forces acting on the patellofemoral joint [23]. Several factors such as "bony alignment, joint geometry, soft-tissue restraints, neuromuscular control, and functional demands" produce abnormally directed loads [24]. These forces exceed the physiological threshold of the tissues and cause symptoms. One of the most consistent anatomic features of patellar malalignment is patella alta [25, 26].

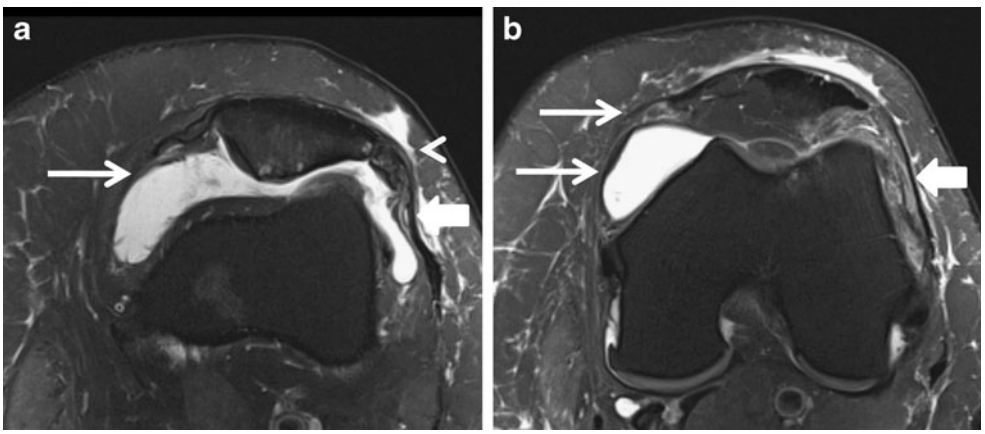

Fig. 16 A 39-year-old woman who was struck by a car as a pedestrian about 15 years ago. Since then she has been having intermittent moderate knee pain. Axial T1-weighted images with fat saturation (**a** and **b**) show an attenuated MPR (*thin arrows*) and a thickened LPR (*thick arrows*)

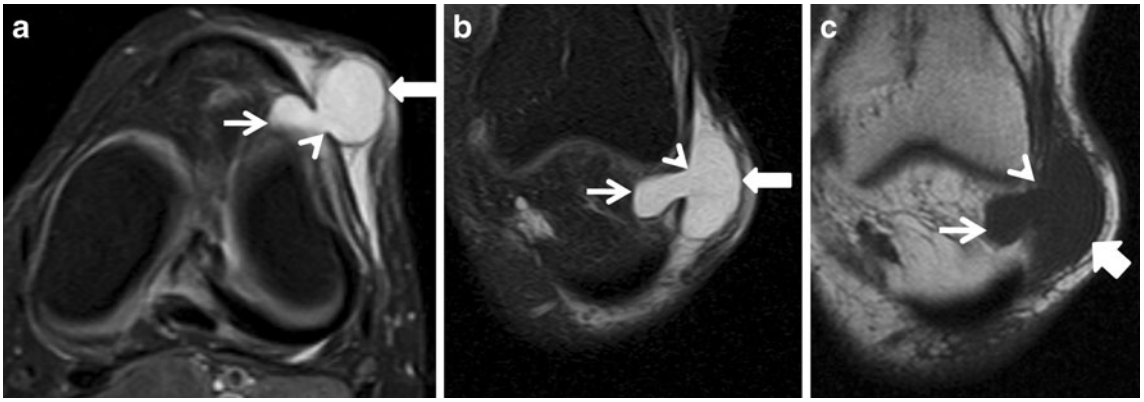

Fig. 17 A 41-year-old woman underwent MRI to evaluate a lump on knee. Axial proton density image with fat saturation (**a**), coronal proton density image with fat saturation (**b**), and coronal proton density image without fat saturation (**c**) show a well-circumscribed T1 hypointense/T2 hyperintense structure in the subcutaneous superficial soft tissues of the anterolateral knee (*block arrow*). A smaller portion (*thin arrows*) of this structure extends posteriorly through the lateral retinaculum into Hoffa's fat pad and the intercondylar notch. The defect in the lateral retinaculum is demonstrated (*arrowheads*). These findings represent a lateral retinaculum diverticulum related to prior injury

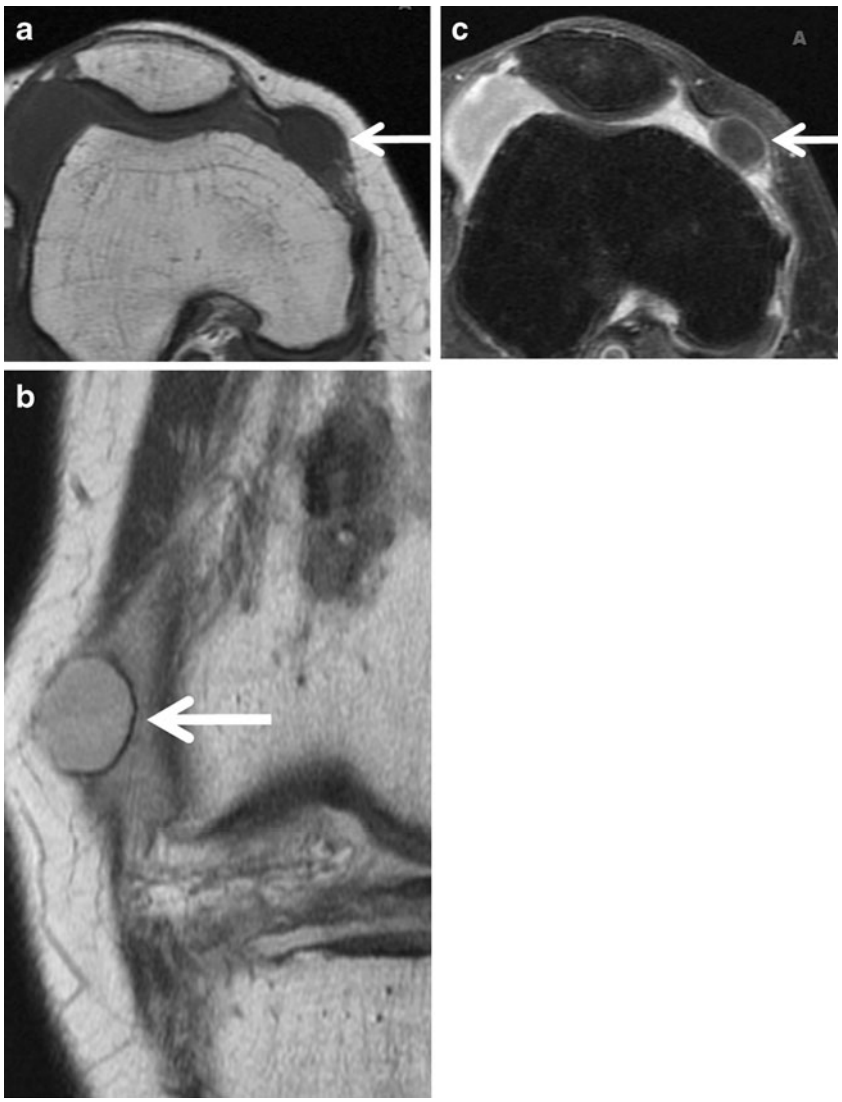

Fig. 18 A 54-year-old woman with polyostotic fibrous dysplasia. Axial (**a**) and coronal (**b**) proton density images show a T1 hypointense cystic mass adjacent to medial retinaculum. Axial T1-weighted image with fat saturation after intravenous gadolinium (**c**) show the mass to be nonenhancing. The mass remained stable for over 3 years. Findings are consistent with a ganglion cyst or a benign nonenhancing myxoma. The absence of contrast enhancement makes ganglion cyst more likely as myxomas generally enhance

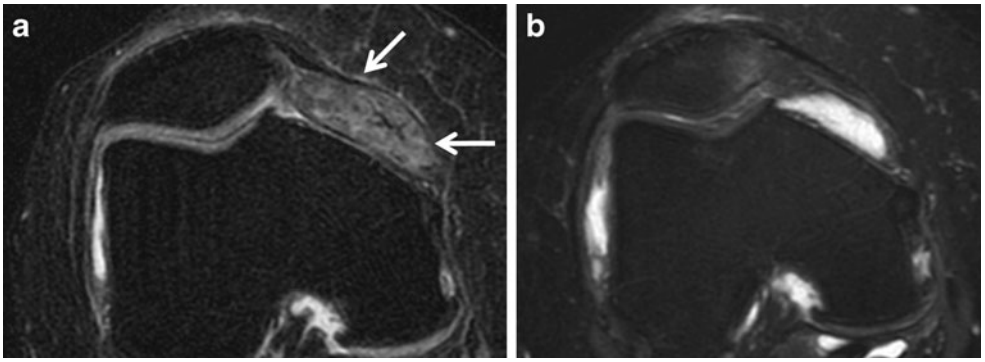

Fig. 19 A 48-year-old woman with right knee pain for 1 year. **a** Axial proton density image with fat saturation shows heterogeneously low signal intensity collection (hematoma) within the medial knee deep to the medial retinaculum. **b** Axial proton density image with fat saturation obtained about 1 year later shows complete resolution

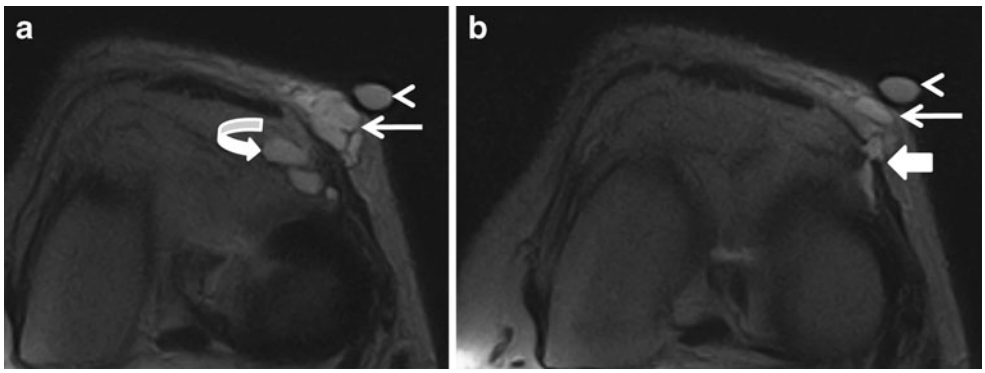

Fig. 20 A 40-year-old man presents with 4 month history of leg pain after running. Low field strength (0.2 T) MRI axial proton density images with fat saturation (**a** and **b**) show a multiloculated lesion (*thin arrows*) within the prepatellar soft tissues subjacent to the skin marker (*arrowheads*). This multiloculated lesion represents a ganglion that insinuates through the lateral retinaculum (*block arrow*). There is another small multilobulated fluid collection within Hoffa's fat pad (*curved arrow*) that represents a parameniscal cyst. The ganglion communicates with the parameniscal cyst through the lateral retinaculum (*block arrow*). Degeneration of the anterior root of the lateral meniscus with a possible tear was also seen (images not shown)

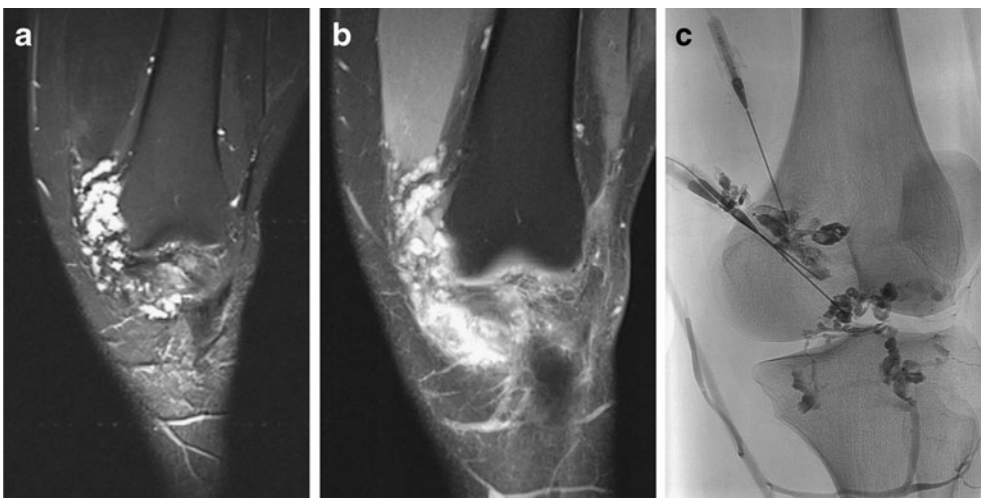

Fig. 21 An example of a venous malformation through the MPR. **a** Coronal T2-weighted image with fat saturation shows serpiginous T2 hyperintense signal along the medial and anterior aspect of the left knee, surrounding the medial retinaculum and extending through the infrapatellar fat pad. **b** Coronal T1-weighted image with intravenous gadolinium shows avid enhancement of this region. **c** Venography demonstrates a moderate venous malformation

Most of the parameters of patellar malalignment are static measurements rather than dynamic. Some examples are tibial tubercle–trochlear groove distance [27], tibial tubercle lateralization and patellar tilt [28], abnormal lateral patellofemoral angle [29], and prefemoral fat pad edema. Edema in superolateral Hoffa's fat pad may also be an important indicator as suggested in a recent study [23]. Trochlear dysplasia causing a shallow trochlear sulcus also predisposes to lateral patellar subluxation. Measurement of lateral trochlear inclination in axial magnetic resonance imaging scans has also been shown to be a good diagnostic criterion [30]. Static parameters as enumerated above fail to evaluate imbalances in the extensor mechanism that include dynamic and neuromuscular factors. In the future, well controlled dynamic–kinematic cross-sectional studies may help in better understanding of the mechanisms of patellofemoral malalignment.

Miscellaneous pathologies

Various additional pathologies may involve the retinacula. Parameniscal cysts (Fig. 19) are postulated to form due to influx of synovial fluid through microscopic and gross tears in the substance of the meniscus [31]. In some cases, the above lesions may become large and envelop the retinaculum, again clinically presenting as a mass lesion. Often, the neck of this multilocular lesion can be traced to the torn meniscus at the joint line level. Venous malformations can be large and multilobular and may infiltrate various layers of the retinaculum (Fig. 20). They typically have bubbly or serpiginous appearance without significant mass effect and are easily distinguished from other neoplastic lesions, with surrounding fat proliferation due to vascular steal phenomenon. Venous malformations, which extend within the joint, are associated with increased frequency of arthropathy (Fig. 21) [32]. Rarely, primary benign and malignant tumors may arise within the retinacular layers, but these lesions show solid or nodular internal enhancement as opposed to the peripheral enhancement observed in the above-mentioned benign lesions, such as ganglion cysts/hematoma/parameniscal cysts. Therefore, intravenous contrast should be used in cases of suspected neoplasm or unusual location/appearance of a cystic looking lesions. Finally, the malignant or synovial lesions may recur along the path of previous surgery.

Conclusion

High-resolution MR imaging readily demonstrates the normal anatomy of the patellar retinacula and enables accurate assessment of the location and grade of injuries to the retinacula and associated structures. Knowledge of the respective imaging patterns of injuries and other retinacular pathologies is essential for patient treatment and prognosis.

References

1. Baldwin JL. The anatomy of the medial patellofemoral ligament. Am J Sports Med. 2009;37(12):2355–61.
2. Merican AM, Amis AA. Anatomy of the lateral retinaculum of the knee. J Bone Joint Surg Br. 2008;90(4):527–34.
3. Merican AM, Sanghavi S, Iranpour F, Amis AA. The structural properties of the lateral retinaculum and capsular complex of the knee. J Biomech. 2009;42(14):2323–9.
4. Amis AA, Firer P, Mountney J, Senavongse W, Thomas NP. Anatomy and biomechanics of the medial patellofemoral ligament. Knee 2003;10(3):215–20.
5. De Maeseneer M, Van Roy F, Lenchik L, Barbaix E, De Ridder F, Osteaux M. Three layers of the medial capsular and supporting structures of the knee: MR imaging-anatomic correlation. Radiographics. 2000;20 Spec No:S83–9.
6. Warren LF, Marshall JL. The supporting structures and layers on the medial side of the knee: an anatomical analysis. J Bone Joint Surg Am. 1979;61(1):56–62.
7. Tuxoe JI, Teir M, Winge S, Nielsen PL. The medial patellofemoral ligament: a dissection study. Knee Surg Sports Traumatol Arthrosc. 2002;10(3):138–40.
8. Starok M, Lenchik L, Trudell D, Resnick D. Normal patellar retinaculum: MR and sonographic imaging with cadaveric correlation. AJR Am J Roentgenol. 1997;168(6):1493–9.
9. Sanders TG, Morrison WB, Singleton BA, Miller MD, Cornum KG. Medial patellofemoral ligament injury following acute transient dislocation of the patella: MR findings with surgical correlation in 14 patients. J Comput Assist Tomogr. 2001;25(6):957–62.
10. Conlan T, Garth Jr WP, Lemons JE. Evaluation of the medial soft-tissue restraints of the extensor mechanism of the knee. J Bone Joint Surg Am. 1993;75(5):682–93.
11. LaPrade RF, Engebretsen AH, Ly TV, Johansen S, Wentorf FA, Engebretsen L. The anatomy of the medial part of the knee. J Bone Joint Surg Am. 2007;89(9):2000–10.
12. Garth Jr WP, Connor GS, Futch L, Belarmino H. Patellar subluxation at terminal knee extension: isolated deficiency of the medial patellomeniscal ligament. J Bone Joint Surg Am. 2011;93(10):954–62.
13. Elias DA, White LM, Fithian DC. Acute lateral patellar dislocation at MR imaging: injury patterns of medial patellar soft-tissue restraints and osteochondral injuries of the inferomedial patella. Radiology. 2002;225(3):736–43.
14. Sanders TG, Paruchuri NB, Zlatkin MB. MRI of osteochondral defects of the lateral femoral condyle: incidence and pattern of injury after transient lateral dislocation of the patella. AJR Am J Roentgenol. 2006;187(5):1332–7.
15. Quinn SF, Brown TR, Demlow TA. MR imaging of patellar retinacular ligament injuries. J Magn Reson Imaging. 1993;3(6):843–7.
16. Diederichs G, Issever AS, Scheffler S. MR imaging of patellar instability: injury patterns and assessment of risk factors. Radiographics. 2010;30(4):961–81.
17. Sillanpaa PJ, Peltola E, Mattila VM, Kiuru M, Visuri T, Pihlajamaki H. Femoral avulsion of the medial patellofemoral ligament after primary traumatic patellar dislocation predicts subsequent instability in men: a mean 7-year nonoperative follow-up study. Am J Sports Med. 2009;37(8):1513–21.

18. Chhabra A, Subhawong TK, Carrino JA. A systematised MRI approach to evaluating the patellofemoral joint. Skeletal Radiol. 2011;40(4):375–87.
19. Chung CB, Skaf A, Roger B, Campos J, Stump X, Resnick D. Patellar tendon-lateral femoral condyle friction syndrome: MR imaging in 42 patients. Skeletal Radiol. 2001;30(12):694–7.
20. Miller PR, Klein RM, Teitge RA. Medial dislocation of the patella. Skeletal Radiol 1991;20(6):429–31.
21. Lemish W, Apsimon T, Chakera T. Lumbar intraspinal synovial cysts. Recognition and CT diagnosis. Spine (Phila Pa 1976) 1989;14(12):1378–83.
22. Soren A. Pathogenesis, clinic, and treatment of ganglion. Arch Orthop Trauma Surg. 1982;99(4):247–52.
23. Subhawong TK, Eng J, Carrino JA, Chhabra A. Superolateral Hoffa's fat pad edema: association with patellofemoral maltracking and impingement. AJR Am J Roentgenol. 2010;195(6):1367–73.
24. Post WR, Teitge R, Amis A. Patellofemoral malalignment: looking beyond the viewbox. Clin Sports Med. 2002;21(3):521–46, x.
25. Simmons E Jr, Cameron JC. Patella alta and recurrent dislocation of the patella. Clin Orthop Relat Res. 1992;(274):265–9.
26. Ward SR, Terk MR, Powers CM. Patella alta: association with patellofemoral alignment and changes in contact area during weight-bearing. J Bone Joint Surg Am. 2007;89(8):1749–55.
27. Balcarek P, Jung K, Ammon J, Walde TA, Frosch S, Schuttrumpf JP, et al. Anatomy of lateral patellar instability: trochlear dysplasia and tibial tubercle-trochlear groove distance is more pronounced in women who dislocate the patella. Am J Sports Med. 2010;38(11):2320–7.
28. Wittstein JR, Bartlett EC, Easterbrook J, Byrd JC. Magnetic resonance imaging evaluation of patellofemoral malalignment. Arthroscopy. 2006;22(6):643–9.
29. Laurin CA, Levesque HP, Dussault R, Labelle H, Peides JP. The abnormal lateral patellofemoral angle: a diagnostic roentgenographic sign of recurrent patellar subluxation. J Bone Joint Surg Am. 1978;60(1):55–60.
30. Keser S, Savranlar A, Bayar A, Ege A, Turhan E. Is there a relationship between anterior knee pain and femoral trochlear dysplasia? Assessment of lateral trochlear inclination by magnetic resonance imaging. Knee Surg Sports Traumatol Arthrosc. 2008;16(10):911–5.
31. Barrie HJ. The pathogenesis and significance of menisceal cysts. J Bone Joint Surg Br 1979;61-B(2):184–9.
32. Jans L, Ditchfield M, Jaremko JL, Stephens N, Verstraete K. MRI demonstrates the extension of juxta-articular venous malformation of the knee and correlates with joint changes. Eur Radiol. 2010;20(7):1792–8.